Investigating Quasar Diversity using UV, X-ray, and Emission-line Properties

Angelica Rivera[1], Gordon T. Richards[1], Ohad Shemmer[2], Sarah Gallagher[3]

1-Drexel University, 2-University of North Texas, 3-Western University

Abstract: We investigate the diversity of quasars through the analysis of their UV (Sheldon et a. 2018), X-ray, and emission-line properties. We concentrate on a sample of 25 radio-quiet SDSS quasars with HST observations that all have similar optical luminosities and redshifts (z~0.5). These objects fill gaps in the sample of "reverberation mapped (RM)" quasars in terms of their CIV parameter space (CIV EQW vs. CIV blueshift). In addition to exploring their UV properties, we use Chandra observations to analyze their X-ray properties (Γ, α_{ox}, $\Delta\alpha_{ox}$), in order to determine how accretion disk winds (which are regulated by α_{ox}) contribute to the diversity of UV emission-line properties in quasars. We compare optical and X-ray derived values of L/L$_{Edd}$, as Γ has been shown to be an indicator of the accretion rate. We are able to determine Γ for 7 quasars from the Chandra sample with over 100 counts. All of the quasars observed with over 100 counts have similar values of α_{ox} and $\Delta\alpha_{ox}$ (averaging ~-1.56 and ~0.42, respectively), while those below 100 counts lie within a wider, weaker range (average α_{ox} ~-1.78, and average $\Delta\alpha_{ox}$ ~0.2). With the combined UV and X-ray data, we explore the differences between quasars and attempt to understand how/when quasars can have high L/L$_{Edd}$, but show little evidence for strong winds.

The Sample: Currently the core "reverberation-mapped" quasars are biased against wind-driven quasars that are more often found at high luminosity (and thus high-z). We use CIV EQW and CIV blueshift to identify a sample that includes such objects and compare their "eigenvector 1" properties such as FWHM Hβ and EQW FeII.

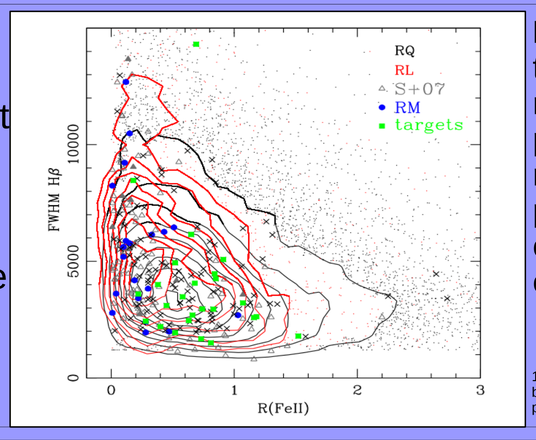

Figure 1: Our targets (green) mapped in EV1 parameter space relative to previously observed RM objects (blue).

1- http://cxc.harvard.edu/cgi-bin/propsearch/prop-details.cgi?pid=4969

The Disk-wind model: Two-component (disk-wind) model of the BELR. UV photons drive the gas by radiation line pressure, and X-rays counteract the process, stripping the gas of electrons (Murray et al. 1995, Richards 2011, Luo et al. 2015, and references therein).

Right: Figure 1 from Murray et al. 1995.

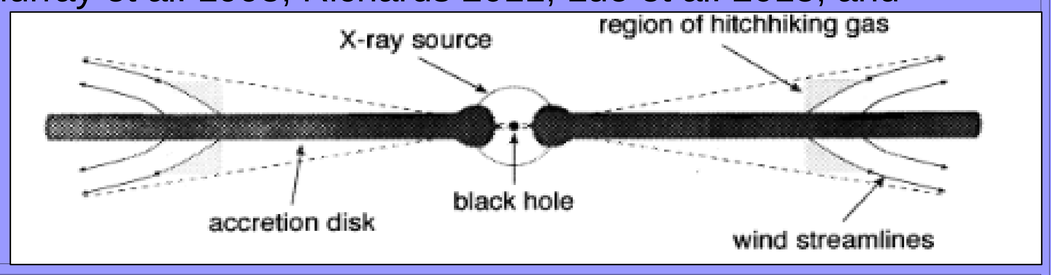

X-ray Properties:

- On average, the X-ray power-law slope Γ is ~2 for quasars (Shemmer et al. 2006).
- α_{ox} is the optical to X-ray spectral index: $\alpha_{ox} = 0.384*\log(L_{2keV}/L_{2500})$
- The relation between L_{2500} and α_{ox} is given by equation (3) from Just et al 2007:

$$\alpha_{ox} = (-0.140 \pm 0.007)*\log(L_{2500})+(2.705 \pm 0.212)$$

- $\Delta\alpha_{ox}$ is the difference between the measured and expected α_{ox} value, and an indicator of X-ray weakness (Gallagher et al. 2006).

Measuring X-Ray Weakness:

- The α_{ox}-LUV relationship has an intrinsic scatter of ~0.15 (1-σ) in α_{ox} units.
- However, $\Delta\alpha_{ox}$ is not sufficient to determine X-ray weakness.
- If the quasar has a very hard spectrum (Γ ≤ 1) and is X-ray weak, the quasar is likely intrinsically absorbed (Gallagher et al. 2006).

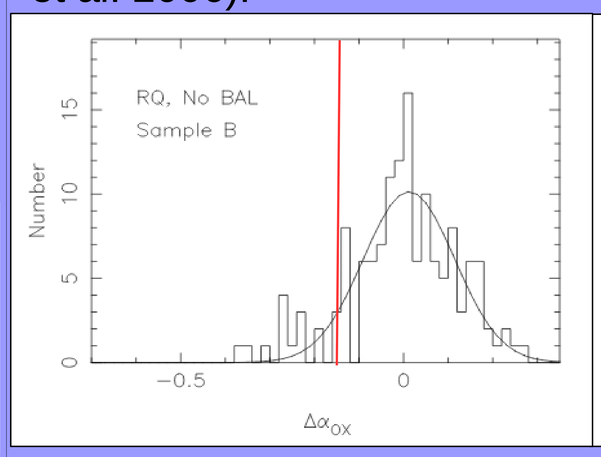

Figure 5: Figure 4 from Gibson et al. (2008). The $\Delta\alpha_{ox}$ distribution for a sample of 139 radio-quiet, non-BAL QSOs. The solid black line is a Gaussian fit, the red line denotes the separation between objects that are greater than 1-σ X-ray weak.

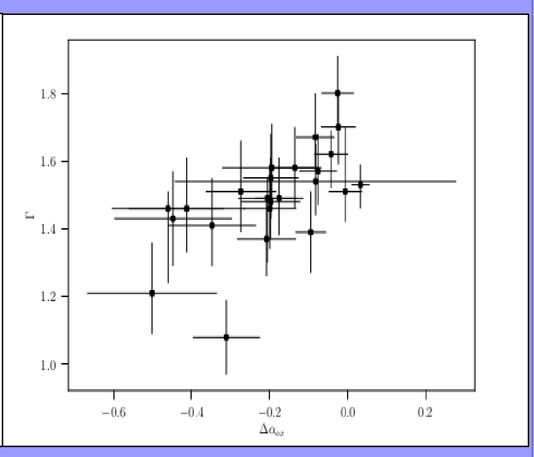

Figure 6: Γ(HR) vs. $\Delta\alpha_{ox}$ for our sample. The Hardness Ratios (HR) were calculated using the Fortran code provided by Park et al. 2006. Γ(HR) was then calculated using the method outlined in Gallagher et al. 2006.

Spectral-Fitting Results: Of our 25 targets only 7 had over 100 full-band counts, despite exposure times being set to obtain 100 counts. This may have been caused by intrinsic absorption affecting the quasars with less than 100 counts.

Table 3. Spectra-fitting Parameters.

SDSS Identifier (1)	fb counts (2)	Spectral Γ (3)	Reduced-χ^2 (4)	N (5)	d.o.f. (6)	Energies Ignored (7)
SDSSJ082024.21+233450.4	$122.9^{+12.1}_{-11.1}$	$2.39^{+0.87}_{-0.65}$	0.90	1.16E-4	11	**-1.36
SDSSJ083332.92+164411.0	$111.6^{+11.6}_{-10.5}$	$1.72^{+0.62}_{-0.51}$	0.89	7.38E-5	12	**-1.37 and bad
SDSSJ093502.52+433110.6	$478.8^{+22.9}_{-21.9}$	$1.62^{+0.28}_{-0.27}$	0.85	3.10E-4	14	**-1.0 5.0-**
SDSSJ112614.93+310146.6	$119.3^{+12.0}_{-10.9}$	$1.98^{+0.41}_{-0.37}$	0.65	7.40E-5	17	**-1.0
SDSSJ113327.78+032719.1	$119.2^{+12.0}_{-10.9}$	$1.96^{+0.52}_{-0.43}$	0.63	7.37E-5	16	**-1.0 6.0-**
SDSSJ123734.47+444731.7	$101.1^{+11.1}_{-10.0}$	$1.93^{+0.62}_{-0.51}$	0.87	6.27E-5	9	**-1.37
SDSSJ125415.55+480850.6	$154.0^{+13.4}_{-12.4}$	$1.86^{+0.77}_{-0.68}$	0.87	1.00E-4	12	**-1.33 5.2-**
SDSSJ134701.54+215401.1	$89.2^{+10.5}_{-9.4}$	$2.43^{+0.82}_{-0.71}$	1.06	6.91E-5	10	**-1.0 5.0-**

The columns are as follows: (1) SDSS J2000 identifier (2) Full-band (0.2-10keV) counts (3) X-ray spectral slope as calculated by XSPEC (4) Reduced-χ^2 statistic (5) 1keV normalization constant (in units of photons/keV/cm^2/s at 1keV) (6) Number of degrees of freedom for the fit (7) Energies ignored during the fitting.
Note that 1-σ errors are given for column (2) and 90% confidence intervals for column (3).

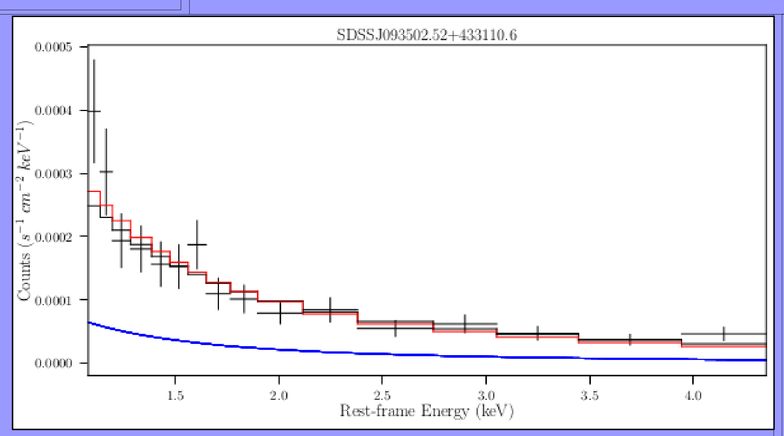

Right: Figures 3 and 4: The best Xspec fits (solid black line) to the spectra for SDSSJ0935+4331 (top) and SDSSJ1126+3101 (bottom) above 2keV rest-frame. In comparison a model fit with Γ=1.8 and galactic absorption is shown in red, a power-law fit with Γ=1.8 is shown in blue.

Future Work: We have the following goals:

1) Compare these specially selected objects to the general population of SDSS quasars with X-ray measurements. (i.e.-Liu et al. 2016, Smith et al., in prep.)

2) Combine the Chandra, UV and optical data to perform a joint analysis of the properties of quasars across EV1 space (e.g.-Shemmer and Lieber 2015).

References: -Arnaud, K., Gordon C., & Dorman, B., 2017, "Xspec: An X-Ray Spectral Fitting Package", 12.9.1, HEASARC/NASA/GSFC, heasarc.gsfc.nasa.gov/xanadu/xspec/XspecManual.pdf, Accessed 3 Mar. 2017 -Chandra X-ray Center, 2016, The Chandra Proposers' Observatory Guide, (Huntsville, Alabama: MSFC) -Dickey & Lockman, 1990, ARAA, 28, 215 Freeman P. E., et al. 2002, ApJS, 138, 185 -Gallagher S. C., et al. 2005, AJ, 129, 567 -Gehrels, N. 1986, ApJ, 303, 336 -Gibson, R.R., et al. 2008, ApJ, 685, 773 -Just, D.W., et al. 2007,ApJ, 665,1004 -Luo, B. et al. 2015, ApJ, 805, 122 -Lyons, L. 1991, A Practical Guide to Data Analysis for Physical Science Students (Cambridge: Cambridge Univ. Press) -Murray et al. 1995, ApJ, 451, 498 -Park, T., et al. 2006, ApJ, 652, 610 -Richards G. T., et al., 2006, ApJS, 166, 470 -Sheldon, K., and Richards, G. 2018, AAS 231, AGN, QSO, Blazars, (Washington D.C.: AAS) -Shemmer, O. et al. 2006, ApJ, 646, L29 -Strateva,I., et al. 2005, AJ, 130, 387

Acknowledgments: Support for this work was provided by the National Aeronautics and Space Administration through Chandra Award Number G07-18110X issued by the Chandra X-ray Center, which is operated by the Smithsonian Astrophysical Observatory for and on behalf of the National Aeronautics Space Administration under contract NAS8-03060. The author thanks Robert Stone.